# SUPPORTING INFORMATION

# In vivo engineering of bone tissues with hematopoietic functions and mixed chimerism

Yu-Ru V. Shih[a], Heemin Kang[a,b], Vikram Rao[a], Roger Yu-Jiu Chiu[b], Seong Keun Kwon[a,c], Shyni Varghese[a,b,1]

[a]Department of Bioengineering, University of California, San Diego, La Jolla, CA 92093, USA.

[b]Materials Science and Engineering Program, University of California, San Diego, La Jolla, CA 92093, USA.

[c]Department of Otorhinolaryngology, Seoul National University Hospital, Seoul, Republic of Korea

[1]To whom correspondence should be addressed. Department of Bioengineering, University of California San Diego, 9500 Gilman Drive, MC 0412, La Jolla, CA 92093, United States.

Phone: +1 858 822-7920

Fax: +1 858 534 5722

E-mail address: svarghese@ucsd.edu (S. Varghese).

## SI Experimental Procedures

### *Synthesis of PEGDA-co-A6ACA hydrogels and macroporous hydrogels*

Poly(ethylene glycol)-diacrylate (PEGDA) ($M_n$=3.4 kDa) and N-acryloyl 6-aminocaproic acid (A6ACA) were synthesized as previously described (1, 2). We prepared macroporous PEGDA-*co*-A6ACA hydrogels using polymethyl methacrylate (PMMA) template leaching method (3). Briefly, a cylindrical mold of 5 mm in diameter was filled with 30 mg of PMMA microspheres (150 - 180 μm in diameter, Bangs Laboratories). Approximately, 20 μL of the precursor solution containing 20% (w/v) PEGDA, 0.5 M A6ACA in 0.5 N NaOH, and 0.3% (w/v) Irgacure (the Photoinitiator) was dispensed into the PMMA microspheres-filled mold and photopolymerized using a UV light source (λ = 365 nm) for 10 min. The PMMA microspheres-loaded hydrogels were incubated in excess acetone for 3 days to dissolve the PMMA components. The resultant macroporous hydrogels measuring 8-mm diameter × 4-mm height (d × h) were hydrated in deionized (DI) water (Fig. S1, Steps 1-3). For 2D experiments involving hydrogel slabs, 1 mm thick hydrogel sheets were prepared, allowed to reach equilibrium in phosphate buffered saline (PBS; pH 7.4) for 48 h, and punched into circular discs of 1 $cm^2$ (area).

### *Biomineralization of hydrogels and macroporous hydrogels*

Biomineralization of the PEGDA-*co*-A6ACA macroporous hydrogels was carried out as described elsewhere (4). The macroporous hydrogels were equilibrated in modified simulated body fluid (m-SBF, pH 7.4) for 6 h. The m-SBF was formulated to contain various ionic components, such as 142.0 mM $Na^+$, 5.0 mM $K^+$, 1.5 mM $Mg^{2+}$, 2.5 mM $Ca^{2+}$, 103.0 mM $Cl^-$, 10.0 mM $HCO_3^-$, 1.0 mM $HPO_4^{2-}$, and 0.5 mM $SO_4^{2-}$ as previously reported (5). The SBF-incubated macroporous hydrogels were immersed in 40 mM $Ca^{2+}$ and 24 mM $HPO_4^{2-}$ solution (pH 5.2) for 30 min and washed using DI water. The macroporous hydrogels were then incubated in m-SBF at 37 °C for 2 days and washed with PBS to yield mineralized macroporous hydrogels (Fig. S1, Step 4).

### *Assembly of dual compartment matrices with differential mineralization*

Synthetic dual compartment matrices with differential mineralization were assembled as described below. The schematic in Figure S1 depicts the experimental procedures. The macroporous nature of the hydrogels is not shown in the schematics after Step 4 for simplicity.

*Mineralized matrices with a macroporous core*: To create a dual compartment matrix containing an outer mineral and inner non-mineral compartment, a modular assembly of mineralized and non-mineralized macroporous hydrogels was employed. Specifically, 3-mm diameter × 4-mm height (d × h) macroporous hydrogels were prepared (*Hydrogel A*; Fig. S1, Step 5a). Mineralized macroporous hydrogels 6 mm × 4 mm (d × h) with an empty core of 3-mm diameter × 4-mm height (d × h) was also created (*Hydrogel B*; Fig. S1, Step 5b). *Hydrogel A* was press-fitted into *Hydrogel B* to create the final 3-D macroporous matrix having a dual compartment structure with a mineralized outer compartment and a non-mineralized inner compartment (Fig. S1, Step 6a). The final matrix of dual compartment structure has a mineralized outer compartment with the dimensions of 6 mm × 4 mm (d × h) and a non-mineralized macroporous inner compartment measuring either 3 mm x 4 mm (d × h) or 1mm x 1mm (d × h). The dual compartment with smaller inner core is termed as BMC-S.

*Mineralized matrices with a hollow core*: To create mineralized macroporous matrices with a hollow core, structures measuring 1-mm diameter and 2.5-mm in depth was punched out from the center of the mineralized macroporous hydrogels (*Hydrogel D*; Fig. S1, Step 5c). A 1.5-mm × 1-mm (d × h) mineralized macroporous hydrogel was used as a cap (*Hydrogel C*; Fig. S1, Step 5c). The capping of the structure (Fig. S1, Step 6b) results in a final matrix containing a mineralized outer compartment with dimensions measuring 6 mm x 4 mm (d × h), and an inner hollow core measuring 1 mm × 1 mm (d × h).

***Scanning electron microscopy (SEM) and energy-dispersive spectroscopy (EDS)***

To evaluate the microstructures of the engineered matrices, SEM imaging was carried out. Briefly, the matrices were rinsed in DI water for 5 min. Samples were sliced into flat pieces and subjected to flash-freezing and lyophilization for 1 day. Iridium coating of the

samples was performed for 7 s using sputter coater (Emitech, K575X) and visualized by SEM (Philips XL30 ESEM). Pore diameters of the matrices were quantified in the dried and swollen states from SEM and bright field images, respectively. The chemical elements of the minerals of the mineralized matrix were determined by EDS analysis using Oxford Energy Dispersive Spectra with INCA software.

***Bone marrow harvest and ex vivo seeding into matrices***

C57BL/6J (CD45.2), B6.SJL-Ptprc$^{a}$ Pepc$^{b}$/BoyJ (CD45.1) and C57BL/6-Tg(UBC-GFP)30Scha/J (Jackson Laboratory, Bar Harbor, ME) mice were bred in the specific pathogen-free area of the institutional animal facility and maintained in a clean region of the facility during the experiments. Two- to three-months-old mice were used for all the experiments. All experiments were approved by the Institutional Animal Care and Use Committee of the University of California, San Diego and were performed in accordance with national and international guidelines for laboratory animal care. For congenic studies, donor bone marrow (BM) (bone marrow cells [BMC] or bone marrow flush [BMF]) from B6.SJL-Ptprc$^{a}$ Pepc$^{b}$/BoyJ (CD45.1) mice were collected and implanted into non-irradiated C57BL/6J (CD45.2) mice. For syngenic studies, donor GFP-positive BM from C57BL/6-Tg(UBC-GFP)30Scha/J mice were implanted into non-irradiated C57BL/6J (CD45.2) mice. For cells implanted in pre-conditioned mice, donor BM from B6.SJL-Ptprc$^{a}$ Pepc$^{b}$/BoyJ (CD45.1) mice were implanted into lethally irradiated C57BL/6J (CD45.2) mice. Mice were sacrificed by cervical dislocation. BM was collected from the femurs and tibia by repeated flushing with Dulbecco's Modified Eagle Medium (DMEM; pH 7.4) supplemented with 0.5% (v/v) bovine serum albumin using a 28-G needle and centrifuged. Prior to loading with bone marrow (BMC or BMF), the sterile matrices were incubated in growth medium containing high glucose DMEM supplemented with 10% (v/v) fetal bovine serum (FBS; Life Technologies, Grand Island, NY), 100 units/mL of penicillin, and 100 μg/mL of streptomycin, for 16 hours. The matrices were air dried for 20 min before loading with BMCs or BMF. BMCs were prepared by repeated pipetting of the BM flush in growth medium to disrupt the cells and ECM. Cells were collected by passing through a cell strainer (40 μm) and centrifuged at 300 rcf. On the other hand, the BMFs were prepared without disturbing the whole BM

and left intact once it was flushed out. The number of CD45-positive hematopoietic cells and CD45-negative non-hematopoietic cells was calculated by using flow cytometry and hemocytometer. Approximately, $5 \times 10^7$ donor hematopoietic BM cells (BMC) in 20 μL of growth medium were loaded into the non-mineralized inner compartment of the macroporous core matrix, while intact whole bone marrow flush (BMF) containing an equal number of hematopoietic CD45 positive cells (~$5 \times 10^7$) were loaded into the central space of matrices containing a hollow core. Non-hematopoietic cells were also loaded along with the hematopoietic cells making the total cells loaded per implant to be ~ $5.2 \times 10^7$ cells. The BMF-loaded matrices (dual compartment structure with a hollow core) were capped with mineralized matrix disk to confine the loaded BMF. Synthetic matrices incorporated with BMF or BMC were kept in growth medium and transplanted into mice within 3 hours (Fig. 1A).

***Subcutaneous implantation of matrices, secondary transplantation, and administration of AMD3100***

Subcutaneous implantation of BMC and BMF-loaded matrices was performed within 3 hrs. Recipient mice were administered with ketamine (100 mg/kg) and xylazine (10 mg/kg), and the fur on the back was shaved. Mice were placed on a heating pad and 1 cm-long incision was made in the back of the mice and a subcutaneous pouch was constructed by blunt dissection using a 1 cm-wide spatula. Vessels in the subcutaneous skin were deliberately cut to expedite vascular formation and anastomosis with the implanted matrices. One matrix was implanted per mice. The skin was sutured after the implantation of BMC- or BMF-laden matrices. After the surgery, all mice were housed in separated cages. For experiments with lethally irradiated mice, matrices were implanted on the same day after mice were irradiated at 10 Gy for 2.5 min. Host chimerism and mobilization of the donor cells were compared against animals that received administration of $5 \times 10^7$ BM cells (CD45 positive cells) through tail vein (TV) or by kidney capsule (KC) implantation. For transplantation of BMC and BMF matrix-derived hematopoietic cells into secondary lethally irradiated mice, donor cells were harvested after 1 month of implantation of BMF- or BMC-loaded matrices. Approximately, $4 \times 10^5$ donor CD45.1 cells were sorted by fluorescence-activated cell sorting (FACS) from

engineered bone and injected along with $2.5 \times 10^5$ competitor CD45.2 cells into lethally irradiated CD45.2 mice. Donor hematopoietic reconstitution was analyzed after 3 months of transplantation. To mobilize hematopoietic progenitors, the chemokine (C-X-C motif) receptor 4 (CXCR4) antagonist, AMD 3100 (Tocris Bioscience, Minneapolis, MN), was administered intraperitoneally at 5 mg/kg.

***Kidney capsule implantation***

Mice were anesthetized with ketamine (100 mg/kg) and xylazine (10 mg/kg), and the fur of the lateral abdomen was shaved. Mice were placed on a heating pad and 1 - 2 cm incision was made to the skin and muscle of the lateral abdomen parallel to the spine. The kidney was exteriorized by gentle pressure outside the muscle wall and the kidney capsule was gently lifted with forceps from the parenchyma of the kidney. A 2 - 4 mm incision of the capsule was made with a fine scalpel. A glass fire-polished pasteur pipette with a rounded closed tip was used to gently open a small capsule pocket for cell implants. A 15 µl volume of DMEM containing ~ $5 \times 10^7$ CD45 positive BM cells was pipetted into the pocket. The kidney was placed back and the muscle wall and skin was closed separately with a single suture (5-0, C-3 vicryl suture).

***Culture and in vitro implantation of human MSCs and HSPCs***

Human mesenchymal stem cells (hMSCs; Texas A&M University) were maintained in growth medium containing high-glucose DMEM, 10% (v/v) fetal bovine serum (FBS; HyClone), 4 mM L-glutamine, and 50 U/mL penicillin/ streptomycin. The cells were passaged at 70% confluence and used for experiments at passages 5-6. Human bone marrow $CD34^+$ hematopoietic stem or progenitor cells (HSPCs) were cultured in STEMSpan SFEMII media supplemented with expansion supplement as recommended by manufacturer's protocol (Stem Cell Technologies). For co-culture on 3-D matrices, $5 \times 10^5$ human HSPCs were mixed with $5 \times 10^5$ human MSCs and seeded into 3-D non-mineralized or mineralized matrices in STEMSpan SFEMII media.

***Isolation and differentiation of mouse MSCs***

Mouse mesenchymal stromal cells (mMSCs) were isolated from femurs and tibiae of 3 month-old C57BL/6J mice as described previously (6). Mice were sacrificed by cervical dislocation. Mice were sprayed with ethanol and the femur and tibiae were obtained. Skin and muscles were removed, and bone marrow was flushed with 28-G needles and discarded. Compact bones were excised and minced into 1 $mm^3$ chips with blades and digested in growth medium (α-MEM containing 10% (v/v) FBS, 4 mM L-glutamine, and 100 U/mL penicillin/streptomycin) supplemented with 1 mg/ml (wt/v) collagenase II (Worthington Biochemical, Lakewood, NJ). Bone chips were digested for 1.5 h on a shaker (DS-500E VWR, Radnor, PA) at 37°C with a shaking speed of 150 r.p.m, washed three times with growth medium and cultured in growth medium for 3 days to allow mMSCs to migrate out. Following 3 days, the media was changed and cultured for additional 3 days. Attached cells were collected by cell scraper and transferred into a new dish with bone chips and cultured for additional 3 days. Cells were passaged at a split ratio of 1:3 and used for experiments at 4-5 passages. For osteogenic differentiation, osteogenic medium was prepared by supplementing growth medium with 10 nM dexamethasone (Sigma– Aldrich), 10 mM β-glycerophosphate (Sigma–Aldrich), and 0.2 mM ascorbic acid (Sigma–Aldrich) (7).

***Micro-computed tomography (μCT) analysis***

To analyze hard tissue formation within the BMC- and BMF-laden matrices, μCT analysis was carried out. Matrices prior to implantation as well as 4 weeks post-implantation were analyzed using μCT. The samples were fixed with 4% paraformaldehyde at 4 °C for 4 days and washed in PBS. Fixed samples were placed in 15-mL centrifuge tubes and tightly sandwiched between styrofoam blocks. The samples were scanned at a resolution of 9 μm/pixel using a μCT scanner (Skyscan 1076; Bruker AXS Inc., Madison, WI). The scanned images were reconstructed using NRecon software (Bruker). The reconstructed images were used to create 3-D images using CTAn software (Bruker) or 2-D transaxial cross-sectional images using DataViewer software (Bruker). To ensure positive signals from minerals, background signals were identically subtracted from the images of all groups by applying the same threshold range of 90-255. Using 3-D images, mineral density was quantified by selecting a minimum of three different areas

from the outer and inner compartments of three different samples and presented as a percentage of bone volume over total volume (BV/TV). Three hundred and sixty degree rotation of 3-D images were generated into movies at approximately 30-degree rotation per second using CTVol software (Bruker).

***Quantitative polymerase chain reaction (qPCR) analysis***

Cells on 2D matrices were directly placed in 1 mL of TRIzol, and their RNA was isolated using a phenol–chloroform extraction method. Osteogenic gene expression including osteopontin (OPN) and bone sialoprotein (BSP) were analyzed by separating outer and inner compartments of engineered bone, crushed with a pestle and immersed separately in 1 mL of TRIzol.

RNAeasy FFPE kit (Qiagen) was used to isolate RNA for cells isolated by FACS following the manufacturer's protocol. One μg of RNA was reverse-transcribed to cDNA using iScript cDNA synthesis kit (Bio-Rad) according to manufacturer's protocol. cDNA solution was mixed with SYBR select master mix (Life Technologies) and primers for Runx2, SP7, osteocalcin, osteopontin, bone sialoprotein, cathepsin K, and 18S rRNA, and analyzed using ABI Prism 7700 sequence detection system (Applied Biosystems). Runx2: TGGCCGGGAATGATGAGAAC (forward), TGAAACTCTTGCCTCGTCCG (reverse); SP7: GCAGCTCAGAGGAGAAGAAGC (forward), TTCTGTGGCGCAAGGAGATT (reverse); osteocalcin: GCTACCTTGGAGCCTCAGTC (forward), AGGGTTAAGCTCACACTGCTC (reverse); Osteopontin: AAACCAGCCAAGGTAAGCCT (forward), TCAGTCACTTTCACCGGGAG (reverse); BSP: TCCACACTTTCCACACTCTCG (forward), CTTTCTGCATCTCCAGCCTTC (reverse); cathepsin K: GCCCTCAAGGTTCTGCTGC (forward), TGGGTGTCCAGCATTTCCTC (reverse); 18S rRNA: ACCAGAGCGAAAGCATTTGCCA (forward), ATCGCCAGTCGGCATCGTTTAT (reverse). The expression for each target gene was normalized to that of corresponding housekeeping gene 18s rRNA and the relative expression was expressed as $2^{-\Delta\Delta C}{}_{\mathrm{T}}$ values.

***Histochemical staining***

For histochemical staining, the implants were collected from mice after 4 weeks implantation. Native murine bone tissue with bone marrow was used as a control. The excised implants and native bone (mice femur) were prepared for paraffin-embedding as described elsewhere (8). Briefly, the samples were fixed in 4% (w/v) paraformaldehyde at 4 °C for 4 days. The fixed samples were demineralized in 10% (w/v) ethylenediaminetetraacetic acid (pH 7.3; Sigma-Aldrich, St. Lois, MO) at 4 °C for 7 days and subsequently washed with PBS. The demineralized samples were dehydrated and equilibrated in Citrisolv (Fisher Scientific, Pittsburg, PA), and incubated in 95% (w/w) paraffin (Thermo Scientific, Waltham, MA) and 5% (w/w) poly(ethylene-*co*-vinyl acetate) (Sigma Aldrich) at 70 °C under vacuum for 1 day. 10 µm–thick paraffin-embedded sections were prepared with a rotary microtome (RM2255; Leica Biosystems, Buffalo Grove, IL).

*H&E staining*: Prior to staining, paraffin was dissolved from the sections by immersing in Citrisolv for 15 min and the sections were re-hydrated. Hydrated sections were immersed in hematoxylin solution (Ricca Chemical Company, Arlington, TX) for 4 min followed by Eosin-Y solution (Thermo Scientific) for 1 min and washed with DI water. Sections were dehydrated and imaged in the color mode under H-filter.

*TRAP staining:* Tartrate-resistant acid phosphatase assay (Sigma-Aldrich) was performed per manufacturer's instructions. Briefly, a working solution was prepared by first mixing 50 µL Fast Garnet GBC Base solution with 50 µL sodium nitrite solution. After 2 min, it was further mixed with 4.5 mL DI water pre-warmed to 37 °C, 50 µL Naphthol AS-Bl phosphate solution, 200 µL acetate solution, and 100 µL tartrate solution. The working solution was added to hydrated sections and incubated for 1 h at 37 °C while protected from light. After 1 h, the sections were rinsed with DI water and immediately imaged in the color mode under H-filter.

*Picrosirius red staining:* Picrosirius red staining was performed according to manufacturer's procedure (Polysciences Inc., Warrington, PA). Rehydrated sections were

placed in Solution A for 2 min, rinsed with DI water, placed in Solution B for 60 min, and then placed in Solution C for 2 min. The stained sections were incubated with 70% ethanol for 45 s, dehydrated, and mounted. Tissue sections were immediately imaged in the color mode under H-filter.

***Immunohistochemical staining***

Decalcified and rehydrated sections were prepared from the excised implants. The sections were treated with a blocking solution containing 3% (w/v) bovine serum albumin and 0.1% (v/v) Triton X-100 at 25 °C for 1 h and incubated with primary antibodies against osteocalcin (1:100; Abcam, Cambridge, MA) or perilipin (1:100; Santa Cruz Biotechnology, Dallas, TX) in a blocking solution at 4 °C overnight. The sections were washed with PBS, treated with 3% (v/v) hydrogen peroxide (Thermo Scientific) for 10 min and washed using PBS, and then incubated with horseradish peroxidase (HRP)-conjugated secondary antibodies (1:200; Jackson ImmunoResearch, West Grove, PA) in a blocking solution at 25 °C for 1 h and washed in PBS. The sections were developed in 3-3' diaminobenzidine peroxidase substrate solution (Vector Laboratories, Burlingame, CA) for 5 min and washed with PBS. The stained sections were imaged with the color mode under H-filter.

***Immunofluorescent staining***

The excised BMC and BMF samples were demineralized and incubated sequentially in 20% (v/v) sucrose (Sigma-Aldrich) in PBS at 4 °C overnight, 50%:50% of OCT (Tissue-Tek® O.C.T. Compound; Sakura, Torrance, CA):20% (v/v) sucrose in PBS at 4 °C overnight, 70%:30% of OCT: 20% (v/v) sucrose in PBS at 4 °C overnight, then 90-100% OCT at 4 °C overnight. All samples were placed on a shaker during incubation. Samples were transferred to a mold and frozen in presence of 2-methylbutane by using liquid nitrogen, and stored at -80 °C until sectioning. The frozen tissue blocks were sectioned with a cryotome cryostat (at -20 °C) to 20-μm thickness. For immunofluorescent staining, sections were treated with 20 μg/mL proteinase K, permeabilized with 0.5% Triton X-100 (4 min, room temperature [RT]), treated with $NABH_4$ (30 min, RT), blocked with 10% (v/v) donkey serum or 3% (v/v) bovine serum albumin (BSA; 30 min, RT) in PBS, and

incubated with CD16/32 (1:100; eBioscience, San Diego, CA). Sections were stained with CD31 [platelet endothelial cell adhesion molecule (PECAM-1); 1:100; Santa Cruz], CD45 (1:100; Santa Cruz), CD150 (1:100; Abcam), CD48-PE (1:50; Abcam), GFP (1:100; Santa Cruz) overnight at 4 °C. As appropriate, secondary antibodies labeled with Allophycocyanin (1:200; Jackson ImmunoResearch), Alexa Fluor 488 (1:200; Thermo Fisher), or Alexa Fluor 546 (1:200; Thermo Fisher) along with Hoechst 33342 (2 μg/mL; Thermo Fisher) were used to bind primary antibodies for 1 h at RT.

Mouse MSCs cultured on 2-D matrices were permeabilized with 0.1% Triton X-100 (5 min, room temperature [RT]), blocked with 3% (v/v) BSA at RT for 1 h in PBS, and incubated with osteocalcin primary antibody (1:100; Abcam) overnight at 4 °C. The next day, samples were incubated with secondary antibody Alexa Fluor 488 (1:200; Thermo Fisher), along with Hoechst 33342 (2 μg/mL; Thermo Fisher) for 1 h at RT. Human HSPCs/MSCs cultured on 2-D matrices were incubated with CD34 primary antibody (1:200; Santa Cruz Biotech) overnight at 4 °C. The next day, samples were incubated with secondary antibody Alexa Fluor 568 (1:200; Thermo Fisher), along with Hoechst 33342 (2 μg/mL; Thermo Fisher) for 1 h at RT. Fluorescence images were acquired using an Olympus FluoView FV100 confocal microscope (Olympus, Center Valley, PA).

***Flow cytometry analyses and FACS***

To analyze hematopoietic cell populations within the engineered bone, the implanted BMC- and BMF-laden matrices were harvested after 1 day, and 4 and 12 weeks of implantation. The excised implants were minced, crushed with a pestle and passed through a 40-μm cell strainer in DMEM supplemented with 3% (w/v) BSA. Hematopoietic cells from native marrow and those implanted in kidney capsule were used for comparison. To determine circulating donor cells, peripheral blood (PB) was harvested from tail vein of mice implanted with the BMC-and BMF-laden matrices, and cells administered via tail-vein injection after 4 and 12 weeks. To analyze AMD 3100-induced mobilization of donor cells, mice implanted with BMC- and BMF-laden matrices and tail vein-injected groups after 4 weeks were used. PB was harvested from tail vein after 1 h of AMD 3100 administration. Red blood cells were lysed with RBC lysis buffer

(eBioscience) for 7 min at RT, filtered with 40-μm nylon filter (BD Biosciences, San Jose, CA), and blocked with mouse IgG for 20 min on ice. HSPCs were characterized for long term-HSC (LT-HSC; $L^-S^+K^+CD150^+CD48^-CD34^-$), short-term HSC (ST-HSC; $L^-S^+K^+CD150^+CD48^-CD34^+$), multipotent progenitors (MPP; $L^-S^+K^+CD150^-CD48^-CD34^+$), common lymphoid progenitors (CLP; $L^-S^{low}K^{low}CD127^+CD34^+$), and common myeloid progenitors (CMP; $L^-S^-K^+CD16/32^-CD34^+$) (9, 10). Cells were stained with antibodies in a buffer containing PBS and 3% (v/v) BSA for 30 min at RT. Antibodies include CD45.1 PE (104), CD45.1 APC (A20), CD45.1 FITC (A20), CD45.2 APC (A20), CD45.2 FITC (104), APC lineage cocktail (BD Pharmingen), Sca-1 PerCP-Cy5.5 (D7), CD117 Alexa Fluor 700 (ACK2), CD150 PE-Cy7 (mShad150), CD48 BV510 (HM48-1) (BD Biosciences), CD34 PE (HM34; Biolegend, San Diego, CA), CD16/32 PE-Cy-7 (93), CD127 PE (A7R34), CD3 FITC (17A2; BD Pharmingen, San Jose, CA), B220 FITC (RA3-6B2; BD Pharmingen), CD11b FITC (M1/70), CD34 FITC (4H11). Endothelial cells were stained with CD31 (MEC 13.3; BD Biosciences). All antibodies were purchased from eBioscience unless otherwise specified. Cells were stained with 4',6-diamidino-2-phenylindole (DAPI) for 5 min to include only live cells and gated for singlets in FSC and SSC. For analysis of apoptotic, necrotic and live cells, propidium iodide (eBioscience) and Hoechst 33342 were added immediately before analysis. Analysis was performed with BD Accuri C6 or BD LSR Fortessa flow cytometers (BD Biosciences) and Flowjo software. To determine *in vivo* hematopoietic repopulating ability of cells from the engineered BMC and BMF groups, $4 \times 10^5$ donor CD45.1 cells were isolated and injected along with $2.5 \times 10^5$ support CD45.2 cells into lethally irradiated CD45.2 mice. Osteoclasts were isolated by a previously described method (11), stained with TRAcP antibody (SPM601; Novus Biologicals) and sorted. Briefly, engineered bone were harvested from mice after 4 weeks, minced and cells were enzymatically released with a mixture of collagenase type 2 (1 mg/mL; Worthington Biochemical, Lakewood, NJ) and trypsin-EDTA (0.12%; Thermo Fisher Scientific) on a shaking incubator for 90 min at 37°C in a 5% $CO_2$ humidified chamber. Released cells were collected by filtering bone chips and supernatant through a cell strainer (40 μm). Cells were washed with growth medium (α-MEM containing 10% (v/v) FBS, 4 mM L-glutamine, and 100 U/mL penicillin/streptomycin), treated with red blood cell lysis

buffer. Harvested cells were fixed with 0.01% formaldehyde for 10 min, permeabilized with 0.5% Tween 20, stained with TRAcP antibody and sorted. All sorting experiments were performed with fluorescence activated cell sorting (BD FACSAriaII).

***Colony formation assay***

Colony formation assay was performed as described by manufacturer's protocol. Cells isolated from BMC and BMF groups were counted and suspended in suspension media composed of α-MEM containing 2% (v/v) FBS, 4 mM L-glutamine, and 100 U/mL penicillin/streptomycin. Approximately, $2.5 \times 10^4$ cells were plated in one well of 6-well plate with 1.1 ml of plating media composed of methocult media (Stem Cell Technologies) and suspension media mixed at 10:1 ratio, and cultured at 37 °C in 5% $CO_2$. Sterile water was placed in a neighboring well to avoid drying of culture over time. Colonies were counted after 10 days of culture.

***Quantification of image intensity***

To quantify the intensity of osteocalcin and picrosirius red staining, images were chosen from multiple sections and random locations of multiple engineered bones ($n$ = 6), converted to 8-bit grayscale images, and their histogram and mean pixel intensity was obtained using *ImageJ* software.

***Statistical analysis***

Beyond the biological replicates, experiments were repeated independently at least twice. Statistical analyses were carried out using Graphpad Prism 5. Two-tailed Student's *t*-test was used to compare two groups. One-way analysis of variance (ANOVA) with Tukey Kramer *post-hoc* test was used to compare multiple groups within the same time point. The *p*-values were obtained from each test.

# SI Figures

**Figure S1**

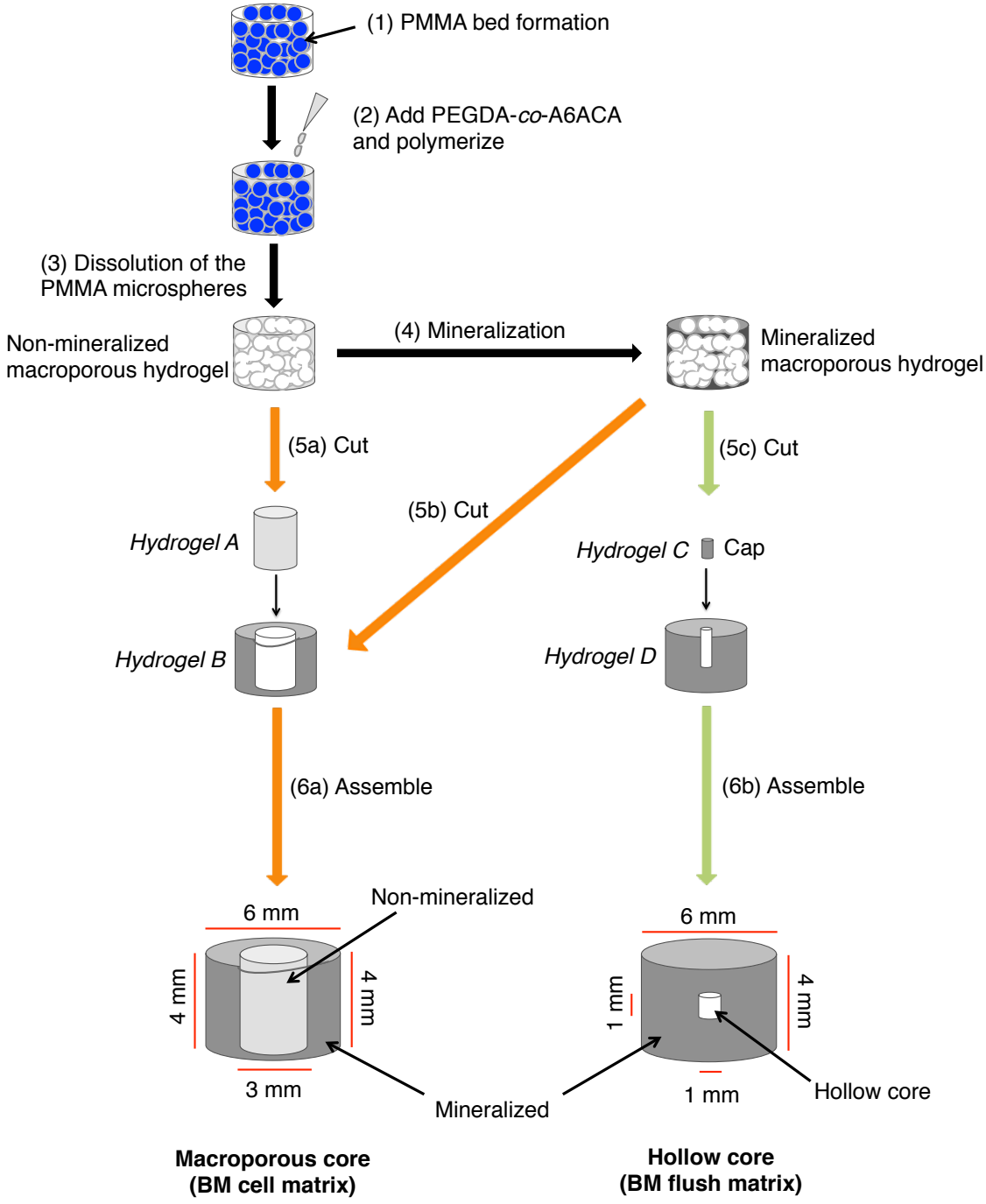


**Figure S1. Schematic depicting the experimental procedures used to manufacture dual compartment synthetic matrices with outer and inner compartments having differential calcification.** Poly(ethylene glycol)-diacrylate-*co*-N-acryloyl 6-

aminocaproic acid (PEGDA-*co*-A6ACA) was polymerized around a polymethyl methacrylate (PMMA) microsphere bed (blue) that was later dissolved to create macroporous hydrogels (Steps 1-3). The pores are enlarged for illustration purposes. Some macroporous hydrogels were further biomineralized to derive mineralized macroporous structures containing calcium phosphate (CaP) moieties (Step 4). Macroporous hydrogels with desired dimensions were cut (Step 5; dimensions are not to scale; pores are not depicted for simplicity) and assembled (Step 6) from non-mineralized and mineralized macroporous hydrogel structures to create dual compartment matrices with either non-mineralized macroporous or hollow core for harboring bone marrow cells (BMC) or bone marrow flush (BMF).

**Figure S2**

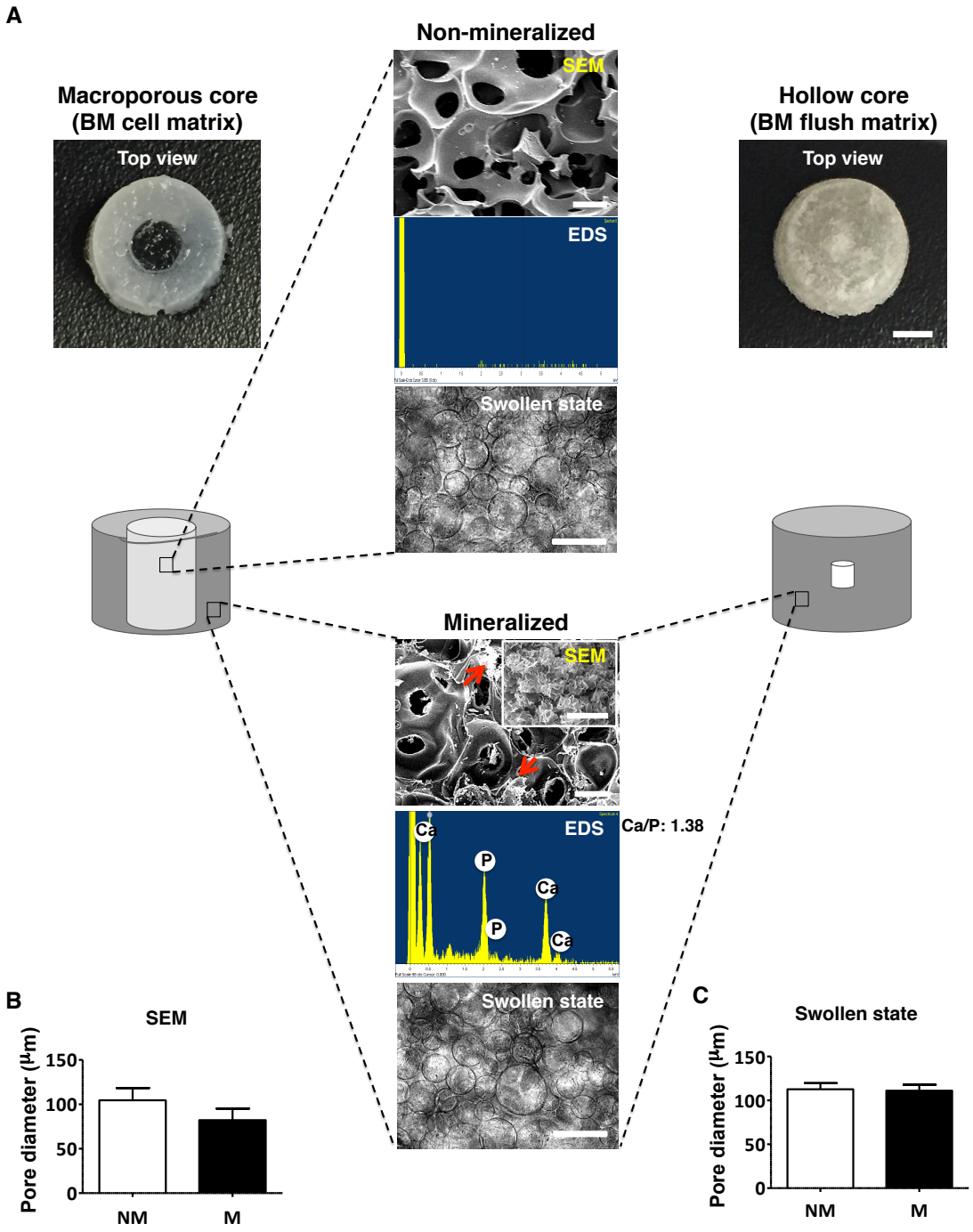


**Figure S2. Characterization of the mineralized and non-mineralized macroporous hydrogels.** (A) Gross image of the dual compartment matrix having a mineralized outer compartment with either a macroporous non-mineralized hydrogel or hollow core in the inner compartment (top view). Scale bar: 2 mm. Scanning electron microscopy (SEM) images of the matrices. Scale bars: 50 μm. The inset shows a high magnification image.

Inset scale bar: 1 μm. Energy dispersive spectroscopy (EDS) shows calcium phosphate (CaP) minerals in mineralized regions (outer compartment) that were absent in the non-mineralized region (inner compartment of BMC matrix). Porous morphology of non-mineralized and mineralized macroporous matrices in their swollen state. Scale bar: 200 μm. Pore diameter of non-mineralized and mineralized compartments in their dry state (B) measured from SEM images and in their swollen state (C) measured from bright field images. Pores were quantified from three random images of four different samples ($n$ = 12). NM: Non-mineralized. M: Mineralized.

**Figure S3**

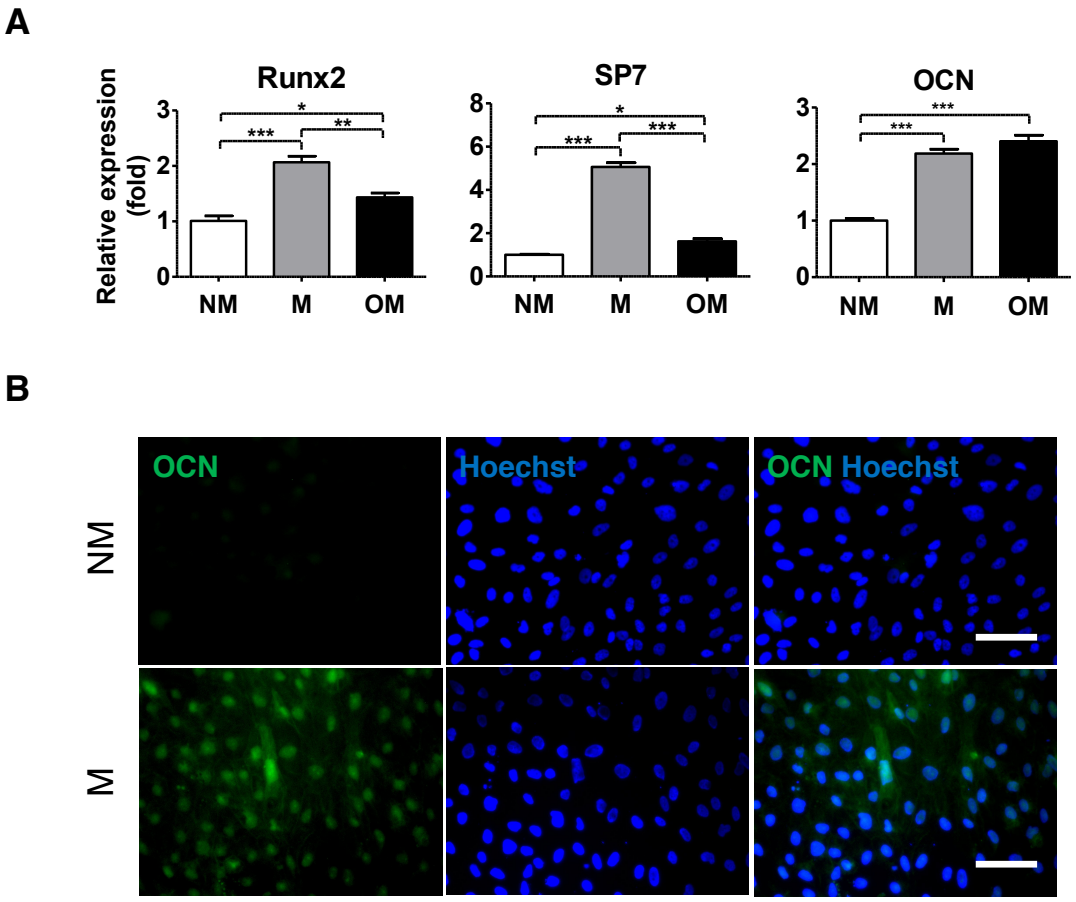


**Figure S3. *In vitro* differentiation of mouse mesenchymal stromal cells on hydrogel matrices.** Mouse mesenchymal stromal cells (mMSCs) were seeded onto two-mineralized and non-mineralized hydrogels (2-D culture) in the absence of osteogenic inducing media and analyzed for (A) osteogenic gene expressions Runx2, SP7 and osteocalcin (OCN), and (B) immunofluorescent staining (green) for osteocalcin . Hoechst (blue) represents nuclear stain. OM: osteogenic medium. Data are presented as mean ± standard errors ($n$ = 6). One-way ANOVA with Tukey *post-hoc* test. *: $p < 0.05$. **: $p < 0.01$. ***: $p < 0.001$. Scale bar: 100 μm.

**Figure S4**

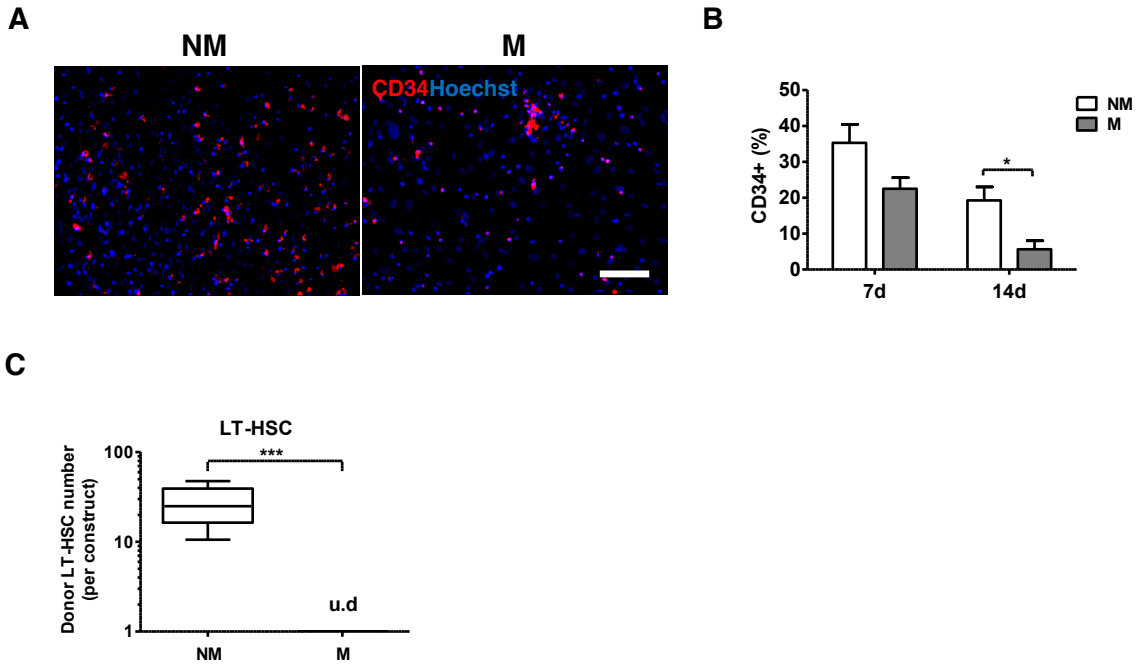


**Figure S4. Maintenance of hematopoietic stem cell population in non-mineralized and mineralized matrices.** (A) Human hematopoietic stem cells (HSCs) and bone marrow-derived mesenchymal stromal cells (MSC) were co-cultured in three-dimensional (3-D) non-mineralized (NM) or mineralized (M) matrices *in vitro* for 7 days and stained for CD34 (red) and nucleus (blue). Scale bar: 200 µm. (B) Percentage of human CD34-positive HSCs after 7 and 14 days of *in vitro* culture. (C) Number of donor CD45.1 long-term hematopoietic stem cells (LT-HSC) in BMC macroporous NM and M matrices after 4 weeks of *in vivo* implantation in congenic CD45.2 mice. u.d: undetectable. Data are presented as mean ± standard errors obtained from multiple samples ($n = 6$). One-way ANOVA with Tukey *post-hoc* test. *: $p < 0.05$. ***: $p < 0.001$.

**Figure S5**

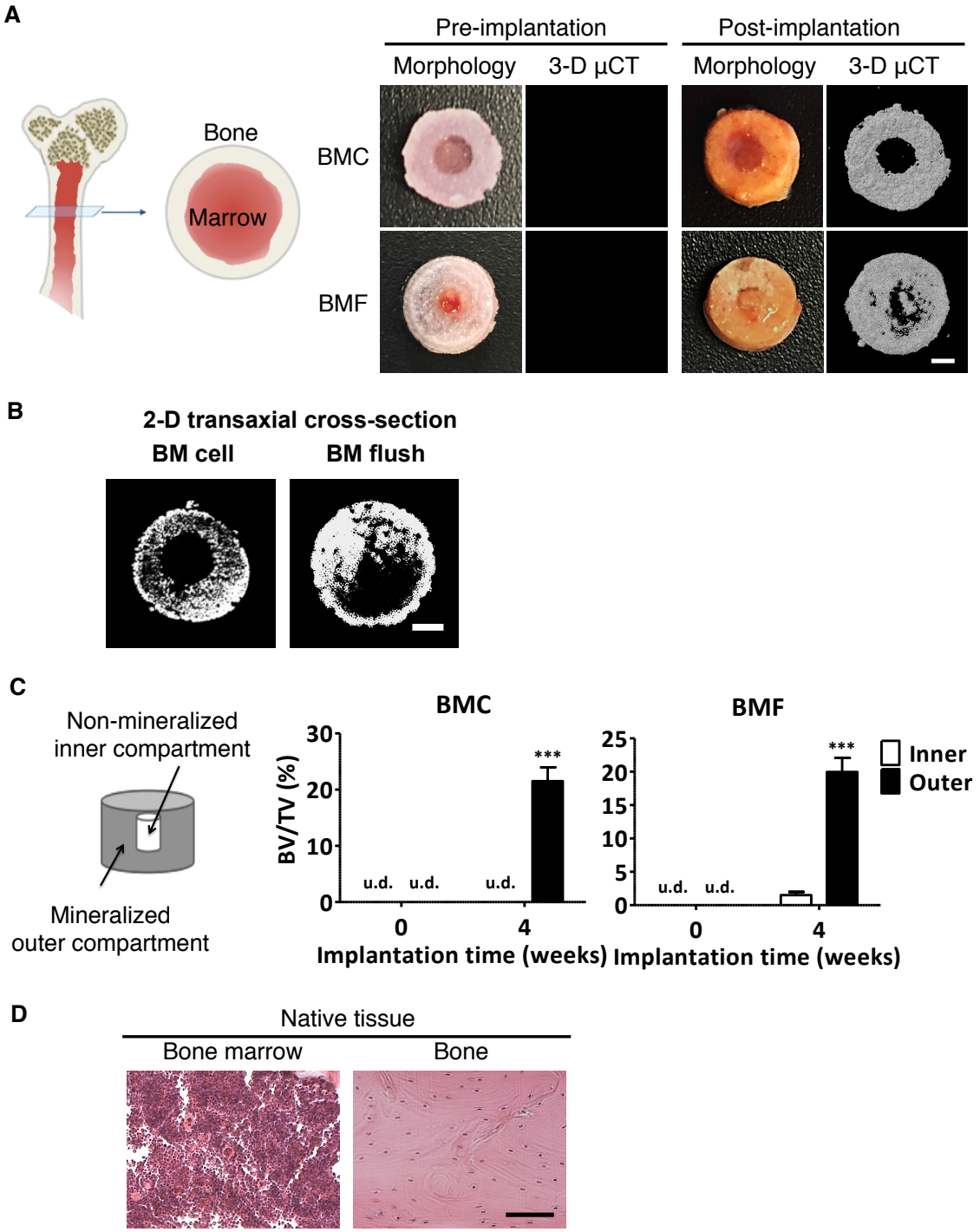


**Figure S5. Characterization of the engineered bone tissues.** (A) Illustration of transverse plane of long bone tissue and gross morphology and 3-D microcomputed tomography (μCT) of CD45.1 BMC- and BMF-laden matrices before transplantation and 4 weeks post-transplantation in congenic CD45.2 mice. Scale bar: 2 mm. (B) Two-

dimensional transaxial cross-section of microcomputed tomography of the engineered bone tissues from matrices loaded with bone marrow cell (BMC) or bone marrow flush (BMF) after 4 weeks *in vivo*. Scale bar: 2 mm. (C) Quantification of percent bone volume estimated from μCT images at the inner and outer compartments of BMC- and BMF-groups. (D) Hematoxylin and eosin stain of native mouse bone with bone marrow. Scale bar: 50 μm. BV/TV: Bone volume/total volume. u.d.: undetected. Data are presented as mean ± standard errors obtained from more than three different samples and three random regions from each sample ($n \geq 9$). Statistical significance was analyzed between inner and outer compartments. Two-tailed Student's *t*-test. ***: $p < 0.001$.

**Figure S6**

**A**

BMC

| | TRAP- | TRAP+ |
|---|---|---|
| **Cathepsin K** | U.D. | 29.49±0.98 |
| **18S rRNA** | 11.46±0.32 | 12.48±0.39 |
| | | Ave. Ct ± SD |

BMF

| | TRAP- | TRAP+ |
|---|---|---|
| **Cathepsin K** | U.D. | 28.46±0.98 |
| **18S rRNA** | 11.73±0.71 | 11.30±0.09 |
| | | Ave. Ct ± SD |

**B**

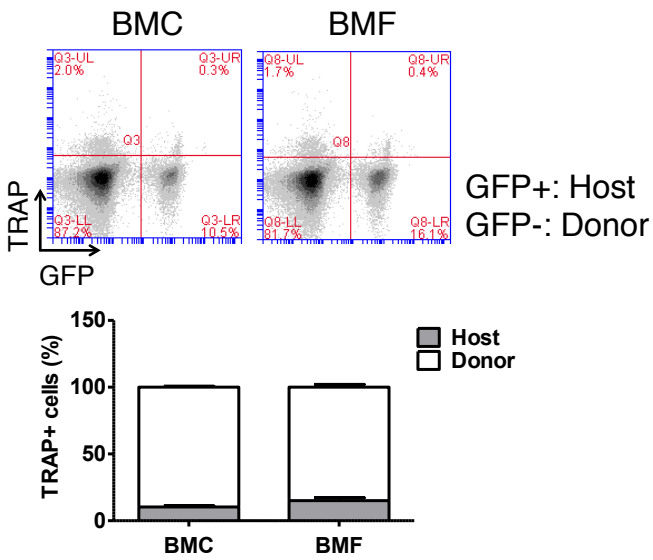


**Figure S6. Characterization of Osteoclasts in engineered bone.** (A) Ct value of cathepsin K gene expression in tartrate resistant acidic protein (TRAP)-positive and TRAP-negative cells in engineered bone. (B) Flow cytometric analyses of donor (GFP-) and host (GFP+) TRAP cells in engineered bone 4 weeks post-implantation.

**Figure S7**

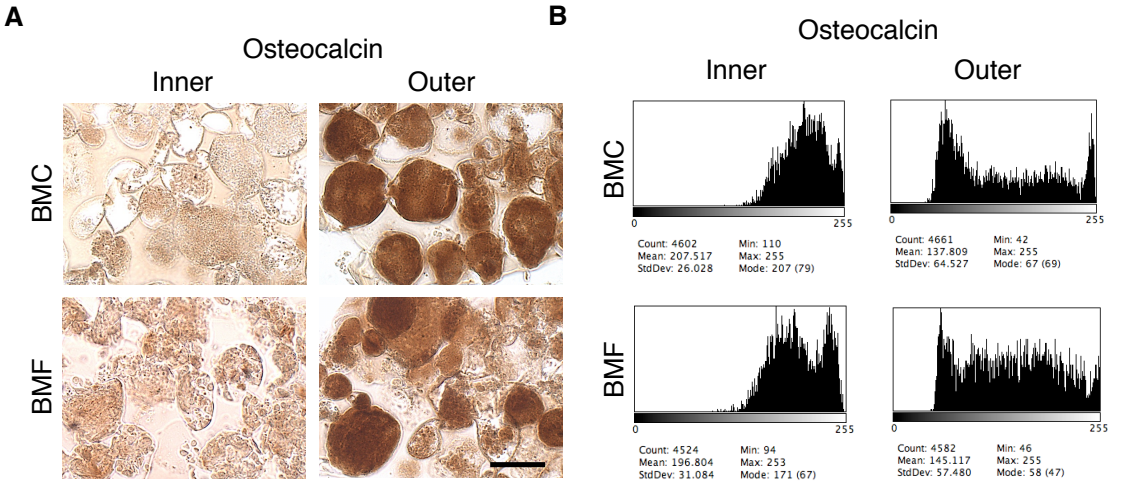


C

Histogram intensity

| | Inner | Outer |
|---|---|---|
| **BMC** | 220.80 ± 11.54 | 162.15 ± 22.18 |
| **BMF** | 194.48 ± 2.01 | 152.42 ± 7.27 |

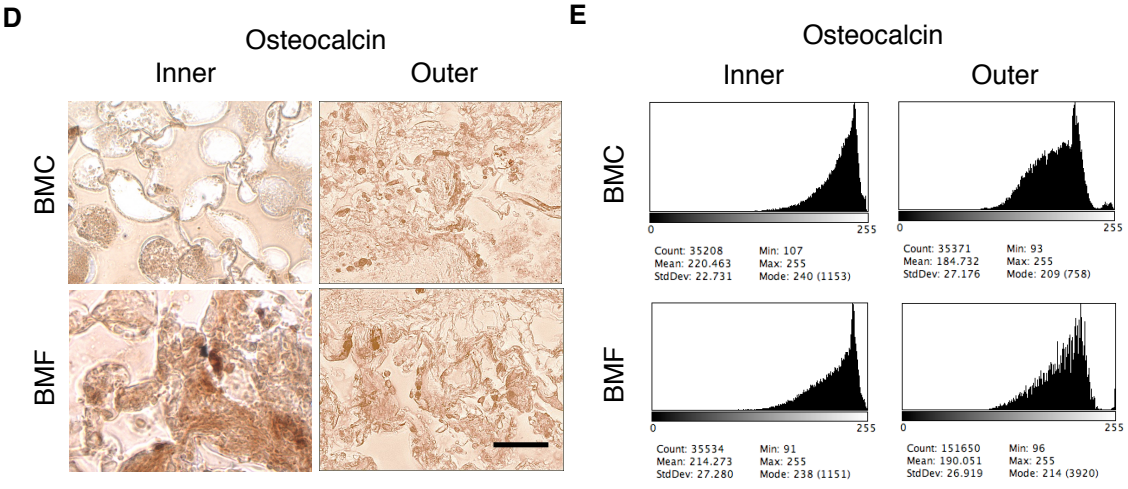


F

Histogram intensity

| | Inner | Outer |
|---|---|---|
| **BMC** | 201 ± 7.13 | 180.55 ± 18.49 |
| **BMF** | 206 ± 19.18 | 189.81 ± 11.64 |

**Figure S7. Osteocalcin staining of the engineered bone and histogram of osteocalcin staining images in the outer and inner compartments of the engineered bone.** (A)

Immunohistochemical staining for osteocalcin, (B) histogram distribution, and (C) quantification of histograms from several samples and images (n=9) after 4 weeks of implantation of BMC- and BMF-laden matrices. (D) Immunohistochemical staining for osteocalcin, (E) histogram distribution, and (F) quantification of histograms from several samples and images (n=9) of osteocalcin 12 weeks postimplantation of BMC- and BMF-laden matrices. Lower histogram values represent higher staining intensity. The immunohistochemical images show the staining intensity at the outer and inner compartments of the engineered bone developed from matrices loaded with bone marrow cell (BMC) or bone marrow flush (BMF). Data are presented as mean ± standard errors. Inner: inner compartment. Outer: outer compartment.

**Figure S8**

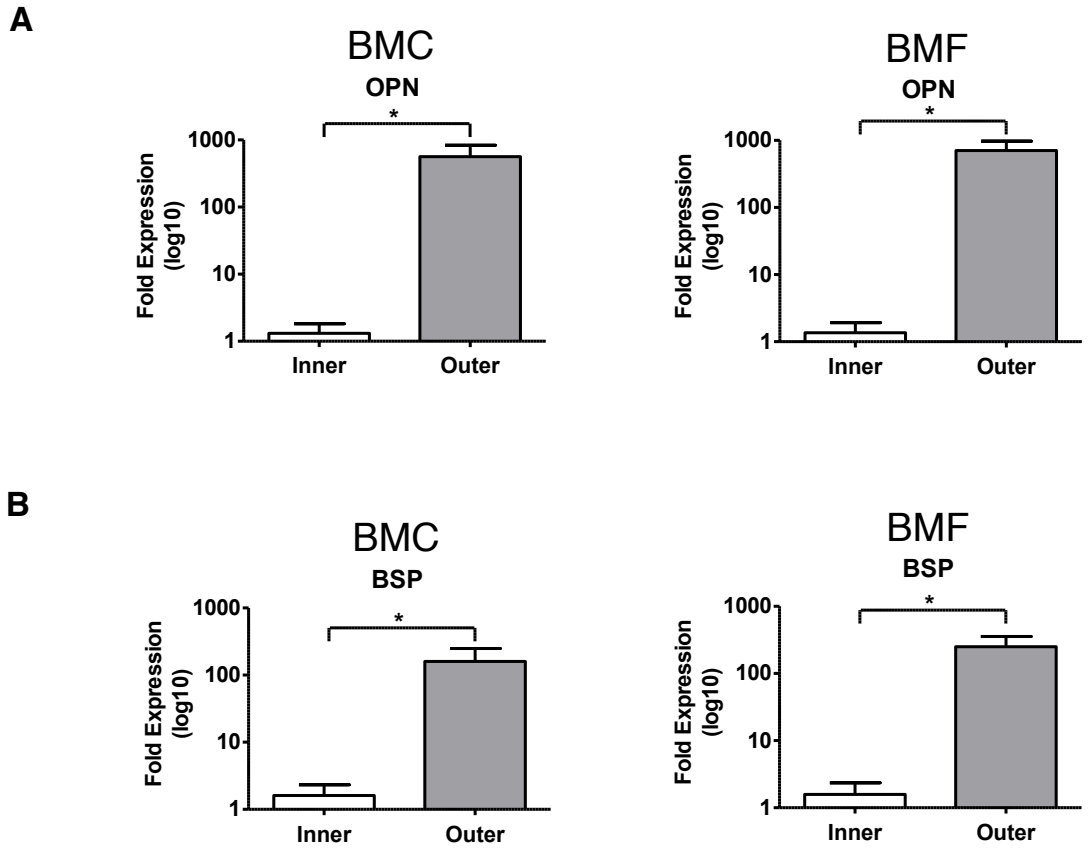


**Figure S8. Characterization of the outer and inner compartments of the engineered bone for different gene markers.** (A) Osteopontin (OPN) and (B) bone sialoprotein (BSP) gene expression in outer and inner compartments of engineered bone 4 weeks post-implantation. Data are presented as mean ± standard errors obtained from three different samples ($n = 3$). Two-tailed Student's $t$-test. *: $p < 0.05$.

**Figure S9**

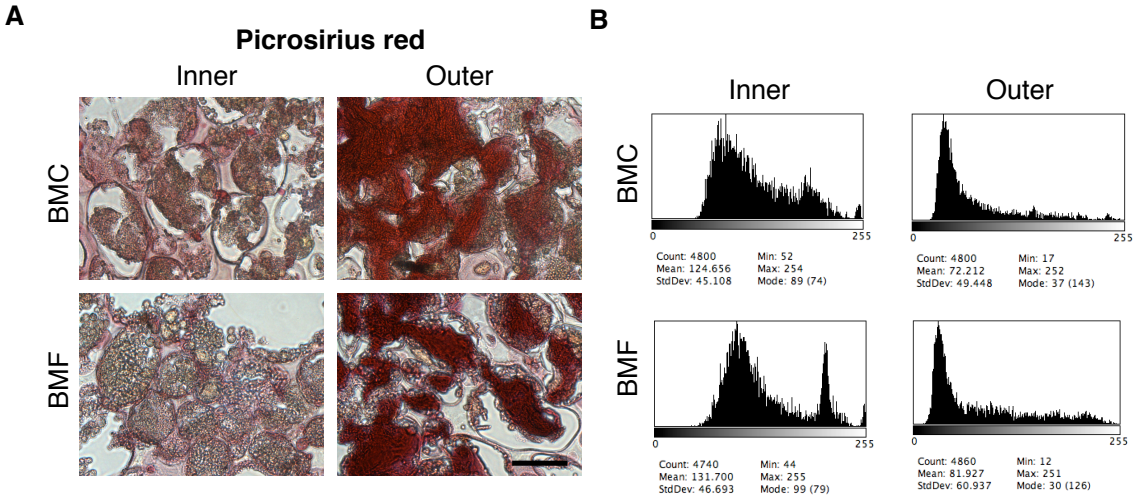


C

Histogram intensity

| | Inner | Outer |
|---|---|---|
| **BMC** | 141.35 ± 30.96 | 92.32 ± 18.10 |
| **BMF** | 134.81 ± 7.48 | 95.24 ± 18.91 |

**Figure S9. Picrosirius red staining of the outer and inner compartments of the engineered bone and the corresponding histogram.** (A) Picosirius red staining, (B) histogram distribution, and (C) quantification of histograms from several images and samples after 4 weeks of implantation. Lower histogram values represent higher intensity. The images show the staining of the outer and inner compartments of the engineered bone developed from matrices loaded with bone marrow cell (BMC) or bone marrow flush (BMF). Data are presented as mean ± standard errors. Pores were quantified from multiple images of different samples ($n$ = 6). Inner: inner compartment. Outer: outer compartment.

**Figure S10**

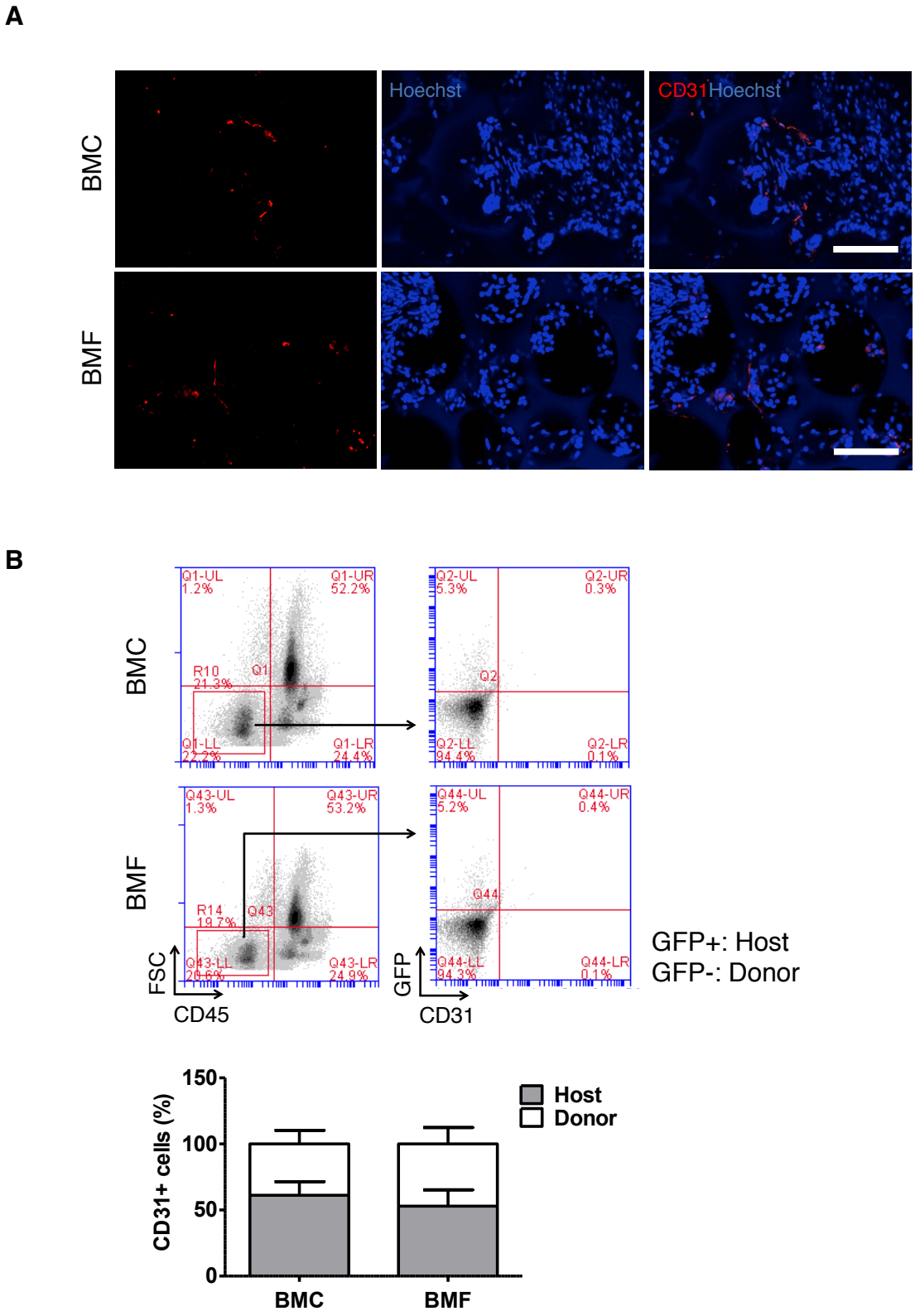


**Figure S10. Vascularization of the engineered bone.** (A) Immunofluorescent staining

for CD31-positive [platelet endothelial cell adhesion molecule (PECAM-1)] endothelial cells (red) 4 weeks post-implantation. Hoechst staining for nucleus (blue). Scale bar: 100 μm. (B) Flow cytometric analyses of donor (GFP-) and host (GFP+) endothelial cells (CD45-CD31+) in engineered bone (both inner and outer compartment) 4 weeks post-implantation. BMC: bone marrow cell constructs. BMF: bone marrow flush constructs.

**Figure S11**

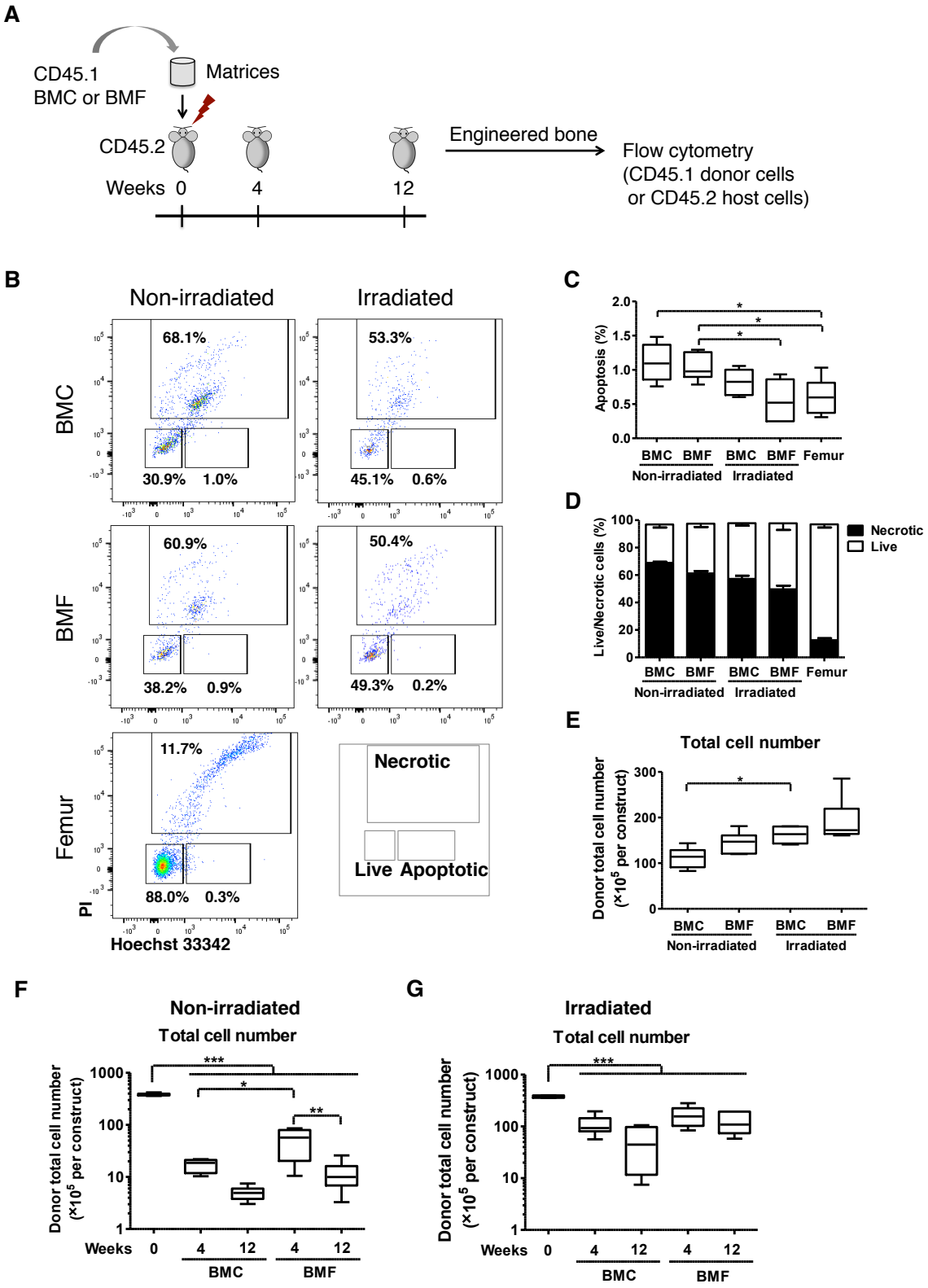
A
CD45.1
BMC or BMF
Matrices
CD45.2
Weeks 0
4
12
Engineered bone
Flow cytometry
(CD45.1 donor cells
or CD45.2 host cells)
B
Non-irradiated
Irradiated
BMC
BMF
Femur
68.1%
30.9%
1.0%
53.3%
45.1%
0.6%
60.9%
38.2%
0.9%
50.4%
49.3%
0.2%
11.7%
88.0%
0.3%
PI
Hoechst 33342
Necrotic
Live Apoptotic
C
Apoptosis (%)
BMC BMF BMC BMF Femur
Non-irradiated Irradiated
D
Live/Necrotic cells (%)
Necrotic
Live
BMC BMF BMC BMF Femur
Non-irradiated Irradiated
E
Total cell number
Donor total cell number (×10^5 per construct)
BMC BMF BMC BMF
Non-irradiated Irradiated
F
Non-irradiated
Total cell number
Donor total cell number (×10^5 per construct)
Weeks 0 4 12 4 12
BMC BMF
G
Irradiated
Total cell number
Donor total cell number (×10^5 per construct)
Weeks 0 4 12 4 12
BMC BMF

**Figure S11. Viability of donor hematopoietic cells in BMC- or BMF-laden matrices immediately after *in vivo* implantation.** (A) Schematic showing experimental procedures. Donor CD45.1-positive bone marrow cell (BMC) or bone marrow flush (BMF) were seeded into matrices and implanted subcutaneously in non-irradiated or lethally irradiated congenic recipient CD45.2 mice respectively. After 1 day, and 4 and 12 weeks, the implants were harvested and analyzed for maintenance of donor (CD45.1) and host (CD45.2) hematopoietic cell populations. (B) Analysis of donor hematopoietic cell survival in bone marrow cell (BMC) and bone marrow flush (BMF)-laden matrices 1 day post-implantation in non-irradiated and lethally irradiated mice. Percentage of (C) apoptotic and (D) live and necrotic cells. (E) Total viable donor hematopoietic cells after 1 day implantation. Absolute number of donor total hematopoietic cells per implant in (F) non-irradiated and (G) lethally irradiated recipient mice. Data are presented as mean ± standard error obtained from six engineered bones ($n = 6$). One-way ANOVA with Tukey *post-hoc* test. *: $p < 0.05$. ***: $p < 0.001$.

**Figure S12**

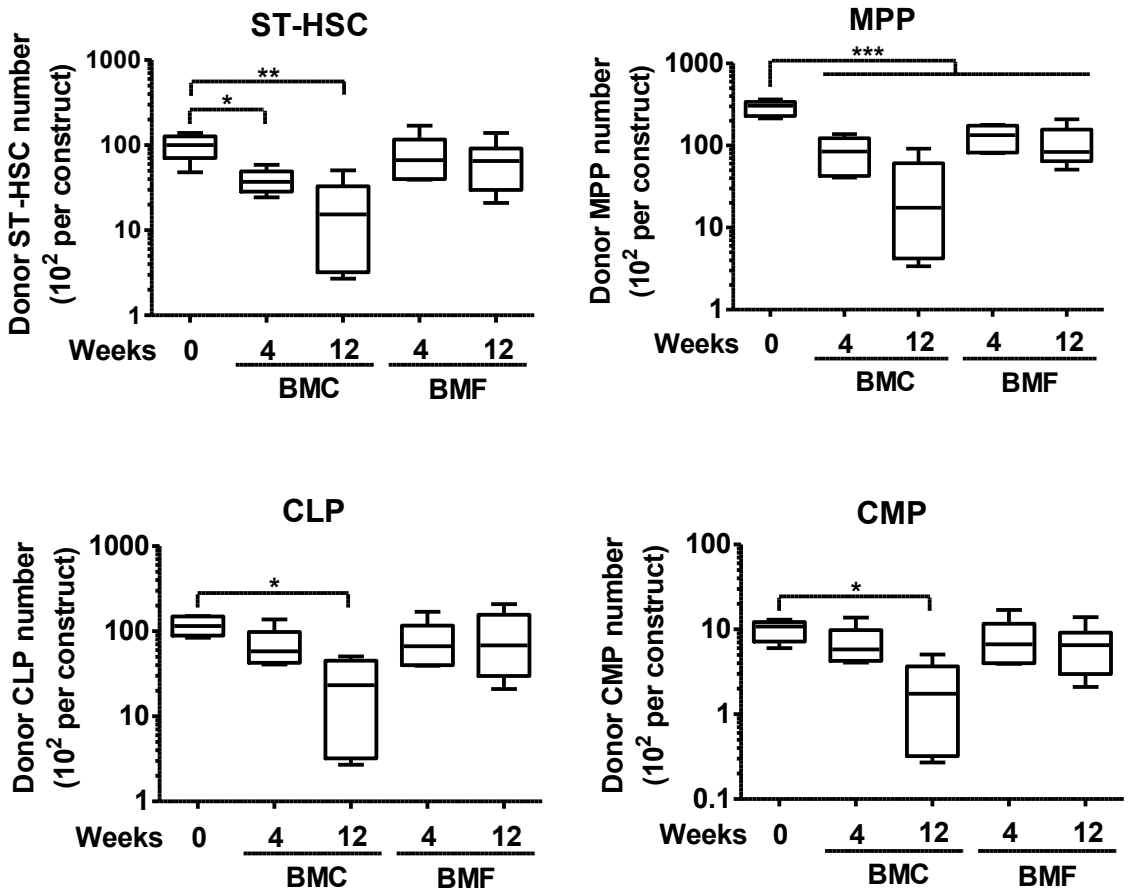


**Figure S12. Donor hematopoietic stem and progenitor cell populations in the engineered bone in lethally irradiated mice.** Donor CD45.1-positive bone marrow cell (BMC) or bone marrow flush (BMF) were seeded into matrices and implanted subcutaneously in lethally irradiated recipient CD45.2 mice. After 4 and 12 weeks, the implants (BMC and BMF groups) were analyzed for donor short-term HSC (ST-HSC), multipotent progenitors (MPP), common lymphoid progenitors (CLP), and common lymphoid progenitors (CMP) within the donor hematopoietic population. Week 0 represents initial cell number. Data are presented as mean ± standard errors obtained from six engineered bones ($n$ = 6). One-way ANOVA with Tukey *post-hoc* test. *: $p < 0.05$. **: $p < 0.01$. ***: $p < 0.001$.

**Figure S13**

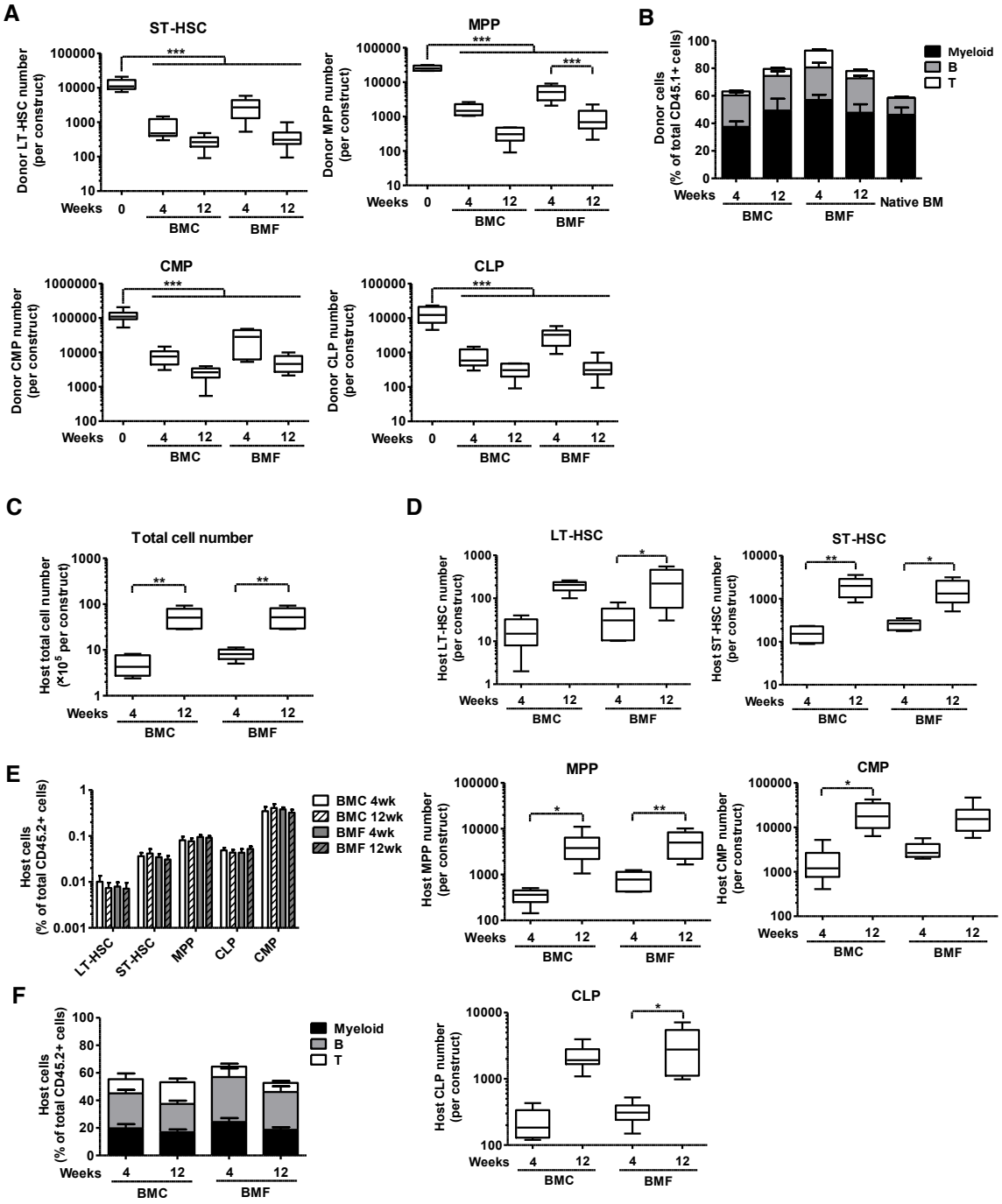


**Figure S13. Donor- and host-mediated hematopoietic cell populations within the engineered bone implanted in non-irradiated congenic mice.** Donor CD45.1-positive bone marrow cell (BMC) or bone marrow flush (BMF) were seeded into matrices and implanted subcutaneously in recipient CD45.2 mice. After 4 and 12 weeks, the implants were harvested and analyzed for maintenance of donor (CD45.1) and host (CD45.2)

hematopoietic cell populations. (A) Absolute number of donor short-term HSC (ST-HSC), long-term HSC (LT-HSC), multipotent progenitors (MPP), common lymphoid progenitors (CLP), and common myeloid progenitors (CMP) for BMC and BMF groups. Week 0 represents initial cell number. (B) Percentage of donor T cell ($CD45.1^+CD3^+$), B cell ($CD45.1^+B220^+$), and myeloid cell ($CD45.1^+CD11b^+$) populations within the donor population of bone marrow cell-(BMC) and bone marrow flush- (BMF) groups. Native BM from mouse femur is used as a control. (C) Total number of host hematopoietic cells. (D) Absolute number and (E) percentage of host long-term HSC (LT-HSC), short-term HSC (ST-HSC), multipotent progenitors (MPP), common lymphoid progenitors (CLP), and common myeloid progenitors (CMP) for BMC and BMF groups. (F) Percentage of host T cell ($CD45.2^+CD3^+$), B cell ($CD45.2^+B220^+$), and myeloid cell ($CD45.2^+CD11b^+$) populations within the donor population of (BMC) and BMF groups. Data are presented as mean ± standard errors obtained from six engineered bones ($n = 6$). One-way ANOVA with Tukey *post-hoc* test. *: $p < 0.05$. **: $p < 0.01$. ***: $p < 0.001$.

**Figure S14**

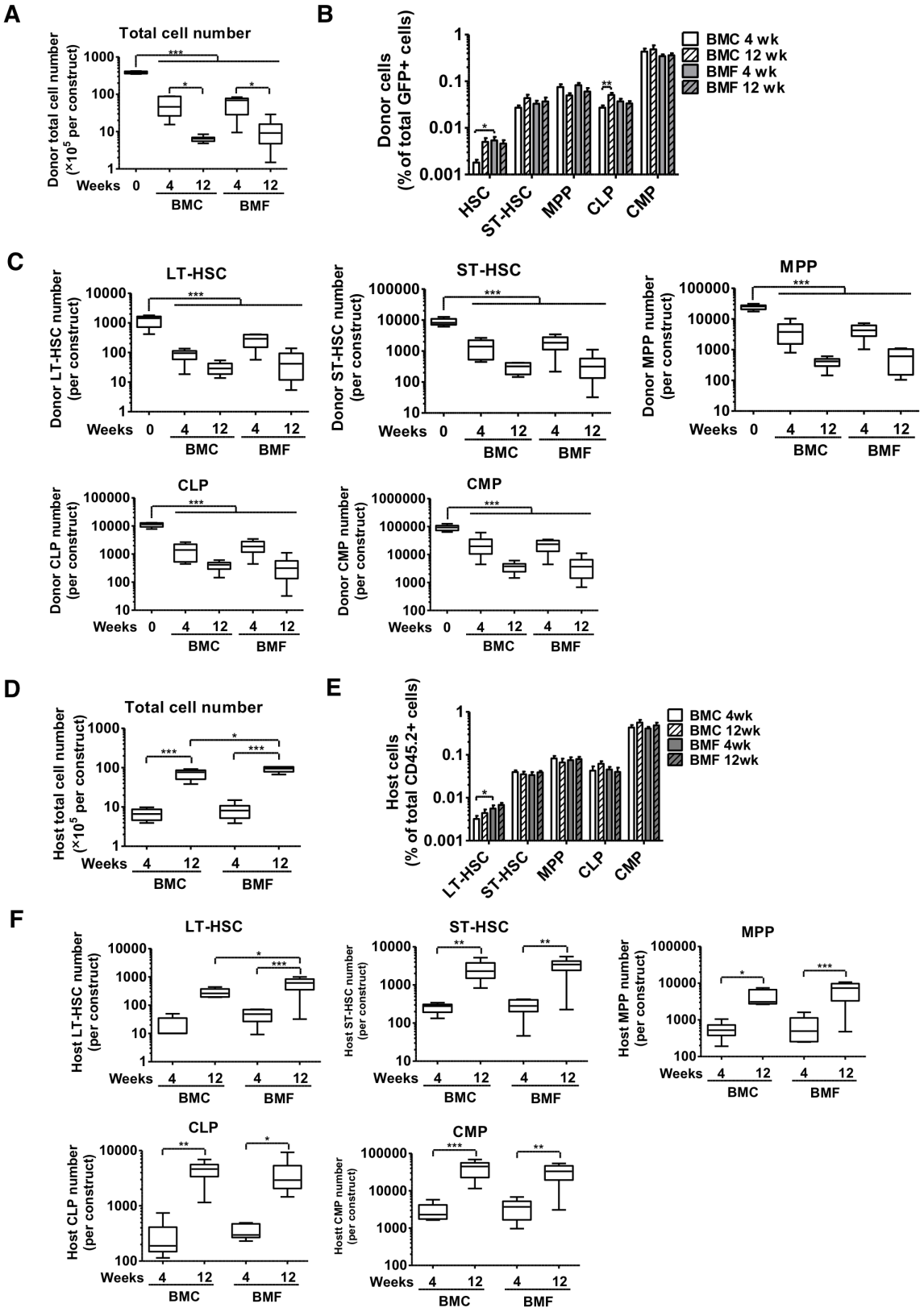
A
Total cell number
Donor total cell number (×10^5 per construct)
Weeks 0 4 12 4 12
BMC BMF
B
Donor cells (% of total GFP+ cells)
BMC 4 wk
BMC 12 wk
BMF 4 wk
BMF 12 wk
HSC ST-HSC MPP CLP CMP
C
LT-HSC
Donor LT-HSC number (per construct)
ST-HSC
Donor ST-HSC number (per construct)
MPP
Donor MPP number (per construct)
CLP
Donor CLP number (per construct)
CMP
Donor CMP number (per construct)
D
Total cell number
Host total cell number (×10^5 per construct)
E
Host cells (% of total CD45.2+ cells)
BMC 4wk
BMC 12wk
BMF 4wk
BMF 12wk
LT-HSC ST-HSC MPP CLP CMP
F
LT-HSC
Host LT-HSC number (per construct)
ST-HSC
Host ST-HSC number (per construct)
MPP
Host MPP number (per construct)
CLP
Host CLP number (per construct)
CMP
Hostt CMP number (per construct)

**Figure S14. Hematopoietic cell populations in engineered bone implanted in non-irradiated syngenic mice.** Donor GFP-positive bone marrow cell (BMC) or bone marrow flush (BMF) were seeded into matrices and implanted subcutaneously in recipient CD45.2 mice. After 4 and 12 weeks, the implants were harvested and analyzed for maintenance of donor (GFP) and host (non-GFP) hematopoietic cell populations. (A) Total number of donor cells. (B) Percent and (C) absolute number of donor long-term HSC (LT-HSC), short-term HSC (ST-HSC), multipotent progenitors (MPP), common lymphoid progenitors (CLP), and common myeloid progenitors (CMP) for BMC and BMF matrices. Week 0 represents initial cell number. (D) Total number of host hematopoietic cells. (E) Percent and (F) absolute number of host long-term HSC (LT-HSC), short-term HSC (ST-HSC), multipotent progenitors (MPP), common lymphoid progenitors (CLP), and common myeloid progenitors (CMP) for BMC and BMF groups. Data are presented as mean ± standard errors obtained from six engineered bones ($n = 6$). One-way ANOVA with Tukey *post-hoc* test. *: $p < 0.05$. **: $p < 0.01$. ***: $p < 0.001$.

**Figure S15**

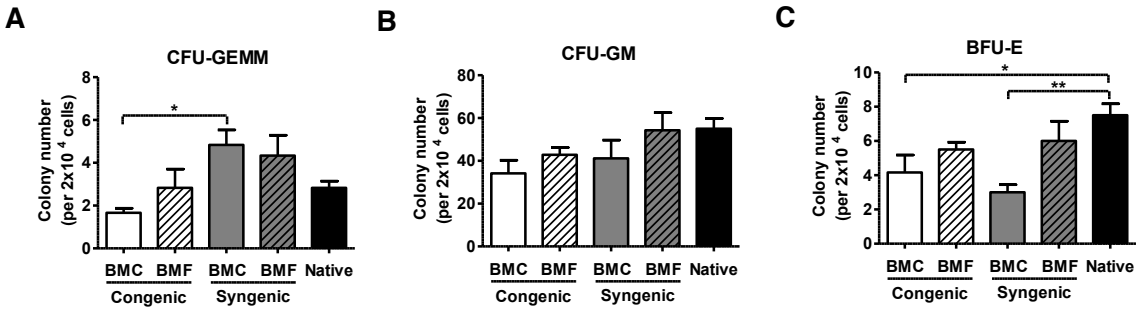


**Figure S15. Colony unit formation of hematopoietic cells derived from engineered bone.** Donor CD45.1-positive bone marrow cell (BMC) or bone marrow flush (BMF) were seeded into matrices and implanted subcutaneously in recipient CD45.2 mice. All cells from the implants were harvested and cultured in methocult, and analyzed for colony formation *in vitro*. Colonies of (A) CFU-GEMM, (B) CFU-GM, and (C) BFU-E cells larger than 50 cells were counted after 9 days of culture. Data are presented as mean ± standard errors obtained from six engineered bones ($n$ = 6). One-way ANOVA with Tukey *post-hoc* test. *: $p < 0.05$. **: $p < 0.01$.

**Figure S16**

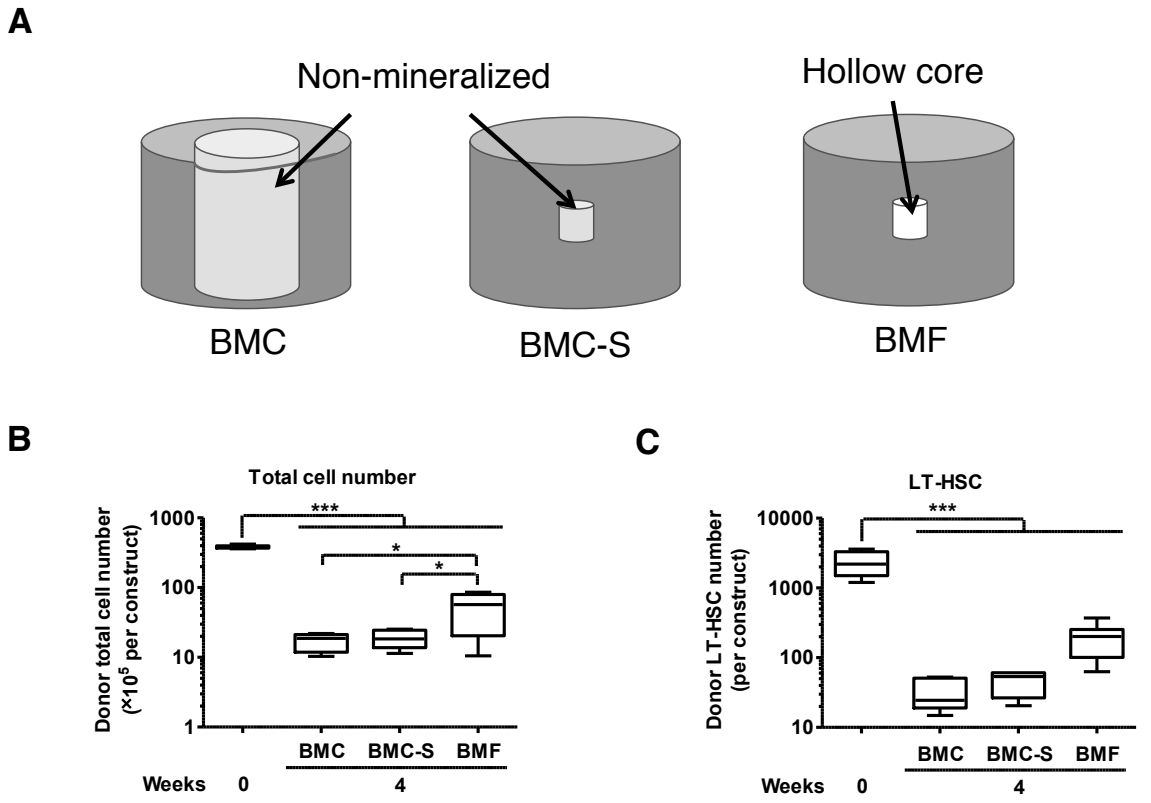


**Figure S16. Effect of dimensions of inner compartment on hematopoietic cell maintenance.** (A) Bone marrow cell (BMC) matrices with the same inner dimensions as those of bone marrow flush (BMF) matrices were made and designated as BMC-S. Donor (CD45.1) bone marrow cells were seeded into BMC, BMC-S and bone marrow flush into BMF matrices and implanted subcutaneously in recipient CD45.2 mice. After 4 weeks, the implants were harvested and analyzed for donor (CD45.1) hematopoietic cell populations. (B) Total donor cell number and (C) LT-HSC number was analyzed from each matrix. Week 0 represents initial cell number. Data are presented as mean ± standard errors obtained from six samples ($n = 6$). Two-tailed Student's t-test was used to compare two groups at the same time point. One-way ANOVA with Tukey *post-hoc* test. *: $p < 0.05$. ***: $p < 0.001$.

**Movie S1**

**Movie S2**

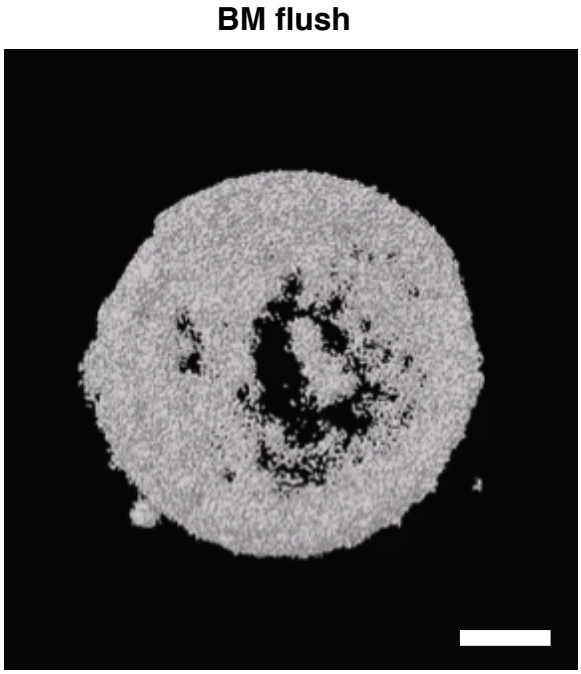

## SI References


1. Ayala R*, et al.* (2011) Engineering the cell-material interface for controlling stem cell adhesion, migration, and differentiation. *Biomaterials* 32(15):3700-3711.
2. Zhang C, Aung A, Liao LQ, & Varghese S (2009) A novel single precursor-based biodegradable hydrogel with enhanced mechanical properties. *Soft Matter* 5(20):3831-3834.
3. Shih YR*, et al.* (2015) Synthetic bone mimetic matrix-mediated in situ bone tissue formation through host cell recruitment. *Acta biomaterialia* 19:1-9.
4. Phadke A, Zhang C, Hwang Y, Vecchio K, & Varghese S (2010) Templated mineralization of synthetic hydrogels for bone-like composite materials: role of matrix hydrophobicity. *Biomacromolecules* 11(8):2060-2068.
5. Oyane A*, et al.* (2003) Preparation and assessment of revised simulated body fluids. *J Biomed Mater Res A* 65A(2):188-195.
6. Zhu H*, et al.* (2010) A protocol for isolation and culture of mesenchymal stem cells from mouse compact bone. *Nat Protoc* 5(3):550-560.
7. Varghese S*, et al.* (2010) Engineering Musculoskeletal Tissues with Human Embryonic Germ Cell Derivatives. *Stem Cells* 28(4):765-774.
8. Lim JI & Lee YK (2009) EVA-enhanced embedding medium for histological analysis of 3D porous scaffold material. *Micron* 40(7):756-760.
9. Wang LD & Wagers AJ (2011) Dynamic niches in the origination and differentiation of haematopoietic stem cells. *Nat Rev Mol Cell Biol* 12(10):643-655.
10. Kiel MJ*, et al.* (2005) SLAM family receptors distinguish hematopoietic stem and progenitor cells and reveal endothelial niches for stem cells. *Cell* 121(7):1109-1121.
11. Benito GE*, et al.* (2002) A new cytometric method for the immunophenotypic characterization of bone-derived human osteoclasts. *Cytometry* 50(5):261-266.